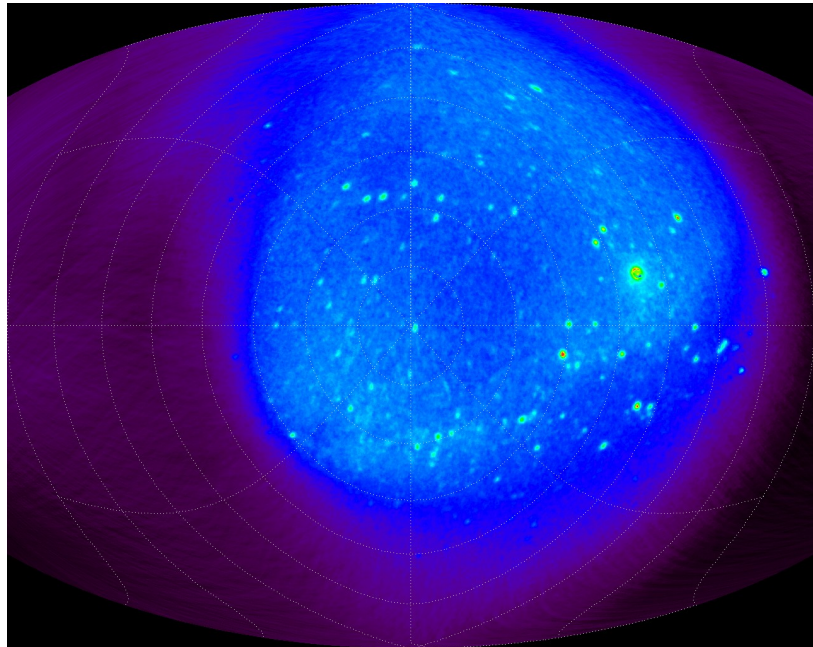


NORSTAR

ASI Mapping



Brian Jackel
Institute for Space Research
University of Calgary

Canadian Space Agency
Contract Report

July 4, 2002

Contents

1 Definitions	4
1.1 Matrix Formalism	4
1.2 Celestial Coordinates	5
1.2.1 Parallax	6
1.3 Geodetic and Geocentric Coordinates	6
1.3.1 Local Orientation	8
1.3.2 The Celestial Pole	9
1.4 Instrument Orientation	9
1.5 Optical System	10
1.5.1 Image Rotation	11
1.5.2 Image Scaling	11
1.6 CCD Pixels	12
2 Data	14
3 Fitting	15
3.1 Initial Values	16
3.2 Quality of Fit	17
3.3 Random Searching	18
3.4 Systematic Optimization	19
4 Viewing Conditions	23
5 Summary	25
5.1 Suggested Implementation	25
6 Additional Information	27
6.1 Jupiter	27
6.2 Bright Stars	29
6.3 IDL Code	30

Introduction

An all-sky imager (ASI) measures the optical intensity of the sky over a wide angular extent. Modern systems use a charge-coupled device (CCD) array detector to record the number of incident photons during a given exposure interval. This grid of measurements is well suited for digital storage and certain kinds of image processing. However, it is ultimately necessary to work in more directly physical coordinates, such as geographic latitude and longitude. Consequently, it is essential to “map” observations from pixel space to other reference frames and coordinate systems.

This report contains a presentation of the concepts and formulae required to carry out several useful transformations. Some practical methods for estimating orientation and instrumental properties are also presented.

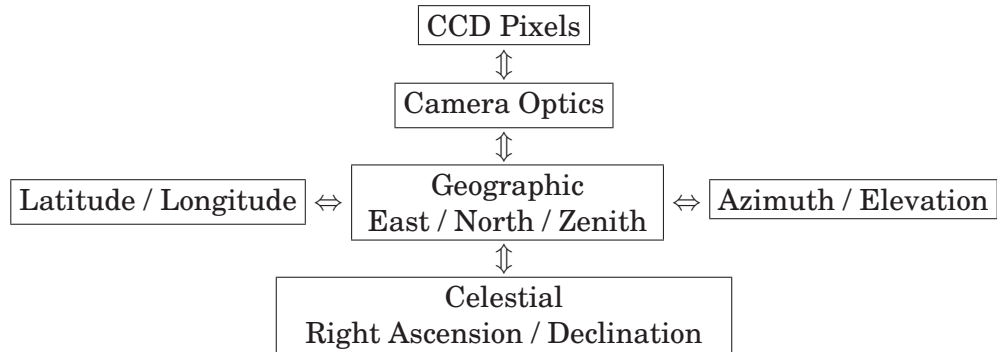


Figure 1: Important coordinate systems for all-sky imagers.

A summary of useful mappings is shown in figure 1. Although scientific application of ASI data only requires conversion from pixel to geographic coordinates, a further transformation to celestial coordinates is extremely helpful for absolute determination of certain quantities. This is due to the fact that all astronomical objects are essentially fixed in the appropriate reference frame. The ability to transform ASI images to the celestial reference frame provides confirmation that all quantities associated with camera optics and orientation are accurately known. Conversely, unknown quantities can be determined by requiring that a sequence of star frames produce the appropriate results (i.e. stationary stars) when transformed to celestial coordinates.

1 Definitions

1.1 Matrix Formalism

The problem of mapping ASI data is essentially two dimensional. A CCD detects photon counts in a planar grid, while incident light may be completely described in terms of zenith angle ζ and azimuth α (or some other pair of angular coordinates). Although the source of luminosity (i.e. the aurora) may have a complex distribution as a function of distance from the imager, none of this information is available from a single frame.

Despite the fundamentally 2-D nature of the problem, it is advantageous to represent orientations in terms of 3-dimensional vectors. For example, the angular direction (ζ, α) can be expressed¹ in Cartesian coordinates

$$x = r \sin \zeta \cos \alpha \quad (1)$$

$$y = r \sin \zeta \sin \alpha \quad (2)$$

$$z = r \cos \zeta \quad (3)$$

which can be inverted to obtain the original angular coordinates

$$\alpha = \tan^{-1} \left(\frac{y}{x} \right) \quad (4)$$

$$\zeta = \tan^{-1} \left(\frac{\sqrt{x^2 + y^2}}{z} \right) \quad (5)$$

regardless of the value for r . Using three Cartesian coordinates to represent orientation requires 50% more storage space than a pair of angular coordinates, but has certain computation advantages. For example, the angle between two vectors is easily determined

$$\cos \gamma = \frac{\mathbf{a} \cdot \mathbf{b}}{|\mathbf{a}| |\mathbf{b}|} \quad (6)$$

More importantly, many useful transformations can be expressed in terms of multiplication with a 3-by-3 matrix

$$\mathbf{a}_2 = \mathbf{T} \mathbf{a}_1 \quad (7)$$

$$\begin{bmatrix} x \\ y \\ z \end{bmatrix}_2 = \begin{bmatrix} T_{11} & T_{21} & T_{31} \\ T_{12} & T_{22} & T_{32} \\ T_{13} & T_{23} & T_{33} \end{bmatrix} \begin{bmatrix} x \\ y \\ z \end{bmatrix}_1 \quad (8)$$

Inverse transforms of this class are easily accomplished by multiplication with the matrix inverse

$$\mathbf{a}_1 = \mathbf{T}^{-1} \mathbf{a}_2 \quad (9)$$

¹This convention is commonly used in physics. However, a different latitude/longitude system (defined in Equations 18) is also used in this report.

where for orthonormal matrices (such as those corresponding to rotations)

$$\mathbf{T}^{-1} = \mathbf{T}^T \quad (10)$$

the inverse is equal to the matrix transpose. Multiple rotations can be accomplished by successive multiplication with the appropriate matrices. When doing this it is important to remember that matrix multiplication is associative

$$(\mathbf{T}_3 \mathbf{T}_2) \mathbf{T}_1 = \mathbf{T}_3 (\mathbf{T}_2 \mathbf{T}_1) \quad (11)$$

but not multiplicative

$$\mathbf{T}_2 \mathbf{T}_1 \neq \mathbf{T}_1 \mathbf{T}_2 \quad (12)$$

1.2 Celestial Coordinates

As noted in the introduction, astronomy is not directly relevant to the problem of relating ASI frames to geographic coordinates. There are, however, benefits to be gained from exploring this topic. Stars in the ASI frames provide an indication that viewing conditions are clear. They can also be used as reference sources to determine camera response and orientation, which are the central topics of this report.

Precisely determining the orientation of astronomical objects relative to a terrestrial observer is not trivial. Fortunately, the requirements for ASI applications are much less demanding than for astronomy. Mapping the entire 180° angle of sky to a 512×512 element CCD produces a fundamental lower resolution limit of approximately 20 arc minutes. In practice, multi-pixel binning may reduce this by another factor of two. Camera optics will also have a non ideal point-spread-function, further limiting the achievable angular resolution. Consequently, the angular accuracy required for this report is no more than approximately 6 arc minutes (0.1°). This will be more than adequate for ASI data while allowing for a considerable simplification in algorithmic complexity.

Complete formula for conversion between celestial and terrestrial coordinates can be found in standard references (for example, Lang [1980]). A simplified version of the necessary equations are presented by Hapgood [1992] in the context of general space physics coordinate conversions. In this notation, conversion from celestial to earth centered coordinates (GEI to GEO) can be expressed as a rotation about the z-axis common to both systems. This rotation is in the plane of the Earth's geographic equator from the first point of Aries² to the Greenwich Meridian. The rotation angle θ is the Greenwich Mean Sidereal Time given by

$$\theta = 100.461 + 36000.770T_0 + 15.04107UT \quad (13)$$

²From Lang [1980]: "Vernal equinox: that point of intersection between the ecliptic and the celestial equator which occurs when the Sun is going from south to north. The equinox has the symbol γ and is sometimes called the first point of Aries."

where T_0 is the time in Julian centuries (36525 days) from 12:00 UT on 1 January 2000 (known as epoch 2000.0) to the previous midnight and UT is the universal time. Conversion of a GEI Cartesian vector into the GEI system is accomplished by multiplication with the rotation matrix

$$\mathbf{T}_1 = \begin{bmatrix} \cos \theta & \sin \theta & 0 \\ -\sin \theta & \cos \theta & 0 \\ 0 & 0 & 1 \end{bmatrix} \quad (14)$$

and the reverse transformation by multiplication with $\mathbf{T}_1^{-1} = \mathbf{T}_1^T$.

1.2.1 Parallax

As given in the 1996 Astronomical Almanac, B61, the corrections for diurnal parallax (due to a displacement for the observer from the center of the earth) of distant objects are

$$\Delta\alpha = \pi(\rho \cos \varphi \sin H \sec \delta) \quad (15)$$

$$\Delta\delta = \pi(\rho \sin \varphi \cos \delta - \rho \cos \varphi \cos H \sin \delta) \quad (16)$$

where ρ is the geocentric distance in units of the Earth's equatorial radius, φ is the geocentric latitude, $H = \theta_0 - \alpha$ is the local hour angle, and π may be calculated from $8''.794$ divided by the geocentric distance of the body in astronomical units. These will be very small corrections and can be neglected in most cases. For the moon (and other very close bodies such as satellites) more precise formulae are required.

1.3 Geodetic and Geocentric Coordinates

Relating ASI measurements to astronomical sources requires only the use of geocentric (earth-centered spherical) coordinates. However, an understanding of geodetic coordinates is required to calculate geocentric site locations from commonly available information and to convert to geographic latitude and longitude.

For the purposes of this report, the term "geocentric" will be used to refer to a Cartesian reference frame with the z-axis aligned with the geographic north pole (Earth's rotation axis) and the x-axis defined by the intersection of the Greenwich Meridian and the geographic equator. The y-axis is then defined by the requirement that the coordinate system be right-handed. It may also be useful to work with spherical coordinates, which will be explicitly defined below.

The term "geodetic" will be used in this report to denote a system which partially accounts for the (slightly) non-spherical shape of the earth. From §24.1 of Jekeli [1985]:

The geoid is the equipotential surface in the earth's gravity field that coincides most closely with the undisturbed mean sea level extended continuously under the continents. The direction of gravity is perpendicular to the geoid at every point. On the earth's surface, this direction is defined by two angles, the astronomical coordinates: The astronomical latitude is the angle Φ , $-90^\circ \leq \Phi \leq 90^\circ$, that the gravity vector forms with the equatorial plane; and the astronomical longitude is the angle Λ , $0^\circ \leq \Lambda \leq 360^\circ$ and positive eastwards, that the plane defined by this vector and the celestial pole forms with Greenwich meridional plane.

The reference ellipsoid is a simple mathematical figure that closely approximates the geoid, historically on a regional basis, but on a global basis for modern requirements. It is a surface of revolution formed by rotating an ellipse about its minor (vertical) axis resulting in an oblate (flattened at the poles) ellipsoid.

Definition of geodetic coordinates requires the adoption of some reference ellipsoid. Two examples are given in table 1; the most useful of these is WGS84, used for GPS satellite positioning systems. It differs only slightly from the International Astronomical Union (IAU) ellipsoids.

	IAU 1976	WGS 84 (GPS)	
semi-major axis	a	6378.140 km	equatorial radius
flattening	f	1/298.257	1/298.257223563
semi-minor axis	b	6356.755 km	$b = a(1 - f)$
eccentricity	e	8.181921×10^{-2}	$1 - e^2 = (1 - f)^2$

Table 1: Parameters for standard reference geoids.

In most cases, values of latitude and longitude are implicitly given in geodetic coordinates, and conversion to geocentric is required before further transformations. The following equations³ relate geocentric (Cartesian and spherical) and geodetic coordinates:

Geocentric Cartesian	Geocentric Spherical	Geodetic Ellipsoidal
$X_{GEO} =$	$R \cos \varphi \cos \lambda$	$= (N + h) \cos \phi \cos \lambda$
$Y_{GEO} =$	$R \cos \varphi \sin \lambda$	$= (N + h) \cos \phi \sin \lambda$
$Z_{GEO} =$	$R \sin \varphi$	$= \left(\frac{b^2}{a^2} N + h \right) \sin \phi$

(17)

Longitude λ is the same in both systems, φ is the *geocentric* latitude for a spherical earth and ϕ is the *geodetic* latitude (geographical latitude on the ellipsoid). R is the

³Note the difference between the convention used here and in §1.1.

spherical earth radius (6371.2 km), h is the local height above the reference ellipsoid, and N is the east-west radius of curvature (which is a function of latitude)

$$N(\phi) = \frac{a^2}{\sqrt{a^2 \cos^2 \phi + b^2 \sin^2 \phi}} \quad (18)$$

The inverse transform is more complicated. The quantity

$$p = \sqrt{X_{GEO}^2 + Y_{GEO}^2} = (N + h) \cos \phi \quad (19)$$

can be directly calculated from Cartesian coordinates, and also provides a useful expression for the geodetic height

$$h(\phi) = \frac{p}{\cos \phi} - N(\phi) \quad (20)$$

Geodetic latitude can be determined by successive approximation of

$$\tan \phi_{(i+1)} = \frac{Z_{GEO}}{p} \left(1 - e^2 \frac{N(\phi_{(i)})}{N(\phi_{(i)}) + h(\phi_{(i)})} \right)^{-1} \quad (21)$$

with a starting value $\phi_0 = \tan^{-1}(Z_{GEO}/p) = \varphi$. In practice this converges after a few iterations.

1.3.1 Local Orientation

The geodetic eastward direction expressed in Cartesian coordinates is easily calculated

$$\widehat{\text{east}} = \frac{\partial}{\partial \lambda} [X, Y, Z]_{GEOC} = [-\sin \lambda, \cos \lambda, 0] \quad (22)$$

as is the zenith (vertical)

$$\widehat{\text{zenith}} = \frac{\partial}{\partial h} [X, Y, Z]_{GEOC} = [\cos \phi \cos \lambda, \cos \phi \sin \lambda, \sin \phi] \quad (23)$$

Direct calculation of the northward vector is less trivial, but can be easily obtained from a cross product

$$\hat{y} = \widehat{\text{north}} = \widehat{\text{zenith}} \times \widehat{\text{east}} = [-\sin \phi \cos \lambda, -\sin \phi \sin \lambda, \cos \phi] \quad (24)$$

Explicitly, the relationship between local geodetic and cartesian geocentric coordinates is given by:

$$\begin{bmatrix} x \\ y \\ z \end{bmatrix}_{geoc} = \begin{bmatrix} -\sin \lambda & -\sin \phi \cos \lambda & \cos \phi \cos \lambda \\ \cos \lambda & -\sin \phi \sin \lambda & \cos \phi \sin \lambda \\ 0 & \cos \phi & \sin \phi \end{bmatrix} \begin{bmatrix} east \\ north \\ zenith \end{bmatrix}_{geod} \quad (25)$$

where as usual the inverse transform is provided by the matrix transpose.

1.3.2 The Celestial Pole

By definition, the GEI vector from the center to the earth towards the celestial north pole is $[0, 0, \infty]$. For observations from other locations, the effect of an offset vector (may have to be included

$$\begin{bmatrix} x \\ y \\ z \end{bmatrix}_{local} = \begin{bmatrix} x \\ y \\ z \end{bmatrix}_{GEI} + \begin{bmatrix} x \\ y \\ z \end{bmatrix}_{position} \quad (26)$$

with local azimuth and elevation determined for the offset vector. This degree of detail is only necessary for celestial objects that are relatively close, as noted in 1.2.1. Consequently, the unit vector pointing towards the celestial pole is very well approximated by $[0, 0, 1]_{gei}$ for any location on the earth. At all times this transforms to $[0, 0, 1]_{geoc}$ which in turn becomes

$$\begin{bmatrix} 0 \\ 0 \\ 1 \end{bmatrix}_{geoc} = \begin{bmatrix} 0 \\ \cos \phi \\ \sin \phi \end{bmatrix}_{geod} = \begin{bmatrix} east \\ north \\ zenith \end{bmatrix}_{geod} \quad (27)$$

so the local azimuth is always zero, and the zenith angle equal to the co-latitude $\bar{\phi} = 90^\circ - \phi$.

1.4 Instrument Orientation

During field installation it is desirable to orient an ASI so that it is pointing vertically and aligned with north at the top of the image. Vertical levelling to a few degrees is easily accomplished. Azimuthal alignment is more difficult, unless orientation of the building or mount system is precisely known. Consequently, some general method of accounting for non-ideal alignment is required.

Starting with a vector in some Cartesian coordinate system $\{x_1, y_1, z_1\}$, it is often useful to carry out a rotation about one axis by some angle ψ to produce the new vector $\{x_2, y_2, z_2\}$. This can be expressed as matrix multiplication by some orthonormal array \mathbf{R}

$$X_2 = \mathbf{R}(\psi, \text{axis}) X_1 \quad (28)$$

Multiple rotations can be accomplished by successive multiplication by the appropriate matrices. The transformation from any given Cartesian coordinate system to another can be achieved by three successive rotations performed in a specific sequence. One common convention uses three *Euler angles* applied to the z_1 , x_2 , and z_3 axes. However, as noted by [Goldstein, 1980, pp 147-148] these systems

... have the drawback that when the primed coordinate system is only slightly different from the unprimed system, [certain angles] become indistinguishable, as their respective axes of rotation... are then nearly coincident. To get around this problem all three rotations are taken around different axes. The first rotation is about the vertical axis and gives the *heading* or *yaw* angle ϕ . The second is about a perpendicular axis fixed in the vehicle and normal to the figure axis; it is measured by the *pitch* or *attitude* angle θ . Finally the third angle is one of rotation about the figure axis of the vehicle and is the *roll* or *bank* angle ψ .

The resulting rotation matrix⁴

$$\begin{aligned} \mathbf{T}_3 &= \mathbf{T}(\psi, x_2) \mathbf{T}(\theta, y_1) \mathbf{T}(\phi, z_0) \\ &= \begin{bmatrix} \cos \theta \cos \phi & \cos \theta \sin \phi & -\sin \theta \\ \sin \psi \sin \theta \cos \phi - \cos \psi \sin \phi & \sin \psi \sin \theta \sin \phi + \cos \psi \cos \phi & \cos \theta \sin \psi \\ \cos \psi \sin \theta \cos \phi + \sin \psi \sin \phi & \cos \psi \sin \theta \sin \phi - \sin \psi \cos \phi & \cos \theta \cos \psi \end{bmatrix} \end{aligned} \quad (29)$$

can be used to transform between two arbitrary coordinate systems X and X' . This is a natural system for ground based work.

An ideally mounted camera would be aligned with the local north, east, and vertical vectors. In practice it is usually possible to orient the camera within a few degrees of vertical, but exact north/south alignment is more difficult, and may be impossible due to physical constraints (i.e. building layout). As well, the CCD alignment may not be consistent with the external camera mounting. Typical values for “yaw” may therefore be large, while “pitch” and “roll” are expected to be small. Hence, the transformation from local geodetic orientation begins with a rotation about the zenith (z_1). This could involve angles as large as $\pm 180^\circ$. Subsequent rotations about the y_2 and x_3 axes are expected to be small if the instrument is nearly level.

1.5 Optical System

Many optical systems, including the NORSTAR ASIs, are circularly symmetric about an “optical axis”. Incoming light rays arrive at some angle γ with respect to the optical axis, and are fully specified in terms of a second polar angle ψ . After passing through the camera optics the ray will exit in some new direction (γ', ψ') .

⁴Care must be taken to avoid typographical errors when coding the full \mathbf{T}_3 matrix. For languages where matrix multiplication is built-in (such as IDL), it may be simpler to construct and multiply the three elementary rotation matrices.

1.5.1 Image Rotation

For the purposes of this report it will be assumed⁵ that the polar angle is reversed ($\psi = -\psi'$) by the camera optics. This is true for many imaging systems in which the output plane is mirrored about the x and y axes. The matrix representation of this effect

$$\mathbf{T} = \begin{bmatrix} -1 & 0 & 0 \\ 0 & -1 & 0 \\ 0 & 0 & 1 \end{bmatrix} \quad (30)$$

is equivalent to a 180° rotation about the optical (z) axis. This could be folded into the instrument frame rotation from the previous section, but for this report will be explicitly included in the optical transformations.

1.5.2 Image Scaling

Changing γ to γ' has the effect of expanding or contracting the solid angle subtended by the image. For an ASI the goal is a reduction of the 2π steradian all-sky field of view onto an angular extent approximately equal to

$$\Omega \approx \frac{L_x \times L_y}{f} \quad (31)$$

where f is the focal length from the optics to the CCD, and L_x, L_y are the CCD dimensions.

A lens that covers a hemispherical field of view (180 degrees) is usually called a fish-eye lens. These lenses have inherent large distortion because it is not possible to form an image of a hemispheric field onto a plane without distortion. This distortion should not be considered as an aberration, but as a necessary result of the projection⁶.

There are five standard projection systems that have been used in fish-eye lens design. One convention for representing these expresses the linear displacement in the image plane r in terms of the system focal length f and initial off-axis angle γ . However, the relationship between r and γ may be highly nonlinear, and not amenable to simple modelling. Consequently, the convention used here expresses the final off-axis angle in terms of linear displacement and focal length

$$\frac{r}{f} = \tan \gamma' \quad (32)$$

⁵Instrument schematics indicate that images should not be reversed, but including a reversal produces small values of yaw for well aligned instruments.

⁶Much of the information in this section was taken from notes provided by Robert Eather of Keo Consultants.

The equations governing the five standard projections are then

$$\tan \gamma' = \tan \gamma \quad \text{normal camera lens} \quad (33)$$

$$= 2 \tan \frac{\gamma}{2} \quad \text{stereographic} \quad (34)$$

$$= \gamma \quad \text{equidistant} \quad (35)$$

$$= \sin \gamma \quad \text{orthographic} \quad (36)$$

$$= 2 \sin \frac{\gamma}{2} \quad \text{equisolid} \quad (37)$$

The left panel of Figure 2 shows all five of these functions in terms of entrance angle and normalized linear displacement.

Almost all commercially available fish-eye lenses for 35 mm and medium format cameras are of the equidistant projection type, so that there is no contraction of the image near the edges. The NORSTAR cameras from KEO Consultants use this optical system. However, a 1999/08/31 fax from Bob Eather contains a plot that is somewhere between equisolid and orthographic. We must expect that in general the mapping function will be non-ideal, and may vary from camera to camera. A test of low-order polynomial approximations to the standard projections was found to be unsatisfactory. Further tests showed that low order rational polynomials were much superior. The simple form

$$\gamma' = \frac{a_1 \gamma}{1 + b_2 \gamma^2} \quad (38)$$

gave fits good to approximately 0.1° while a slightly more complicated form

$$\gamma' = \frac{a_1 \gamma + a_3 \gamma^3}{1 + b_2 \gamma^2 + b_4 \gamma^4} \quad (39)$$

gave maximum errors on the order of 0.01° . The right panel of Figure 2 contains a plot of the errors as a function of angle. These results suggest that equations of the form 38 or 39 should be adequate for approximating the actual camera mapping function.

1.6 CCD Pixels

The detector is assumed to be a rectangular array of size $L_x \times L_y$ with $N_x \times N_y$ rectangular pixels. The pixels will be indexed with integers ranging from $x_{CCD} = 0 \dots N_x - 1$, $y_{CCD} = 0 \dots N_y - 1$. For the purposes of this document we will assume that the pixels completely fill⁷ the CCD and thus have dimensions $d_x = \frac{L_x}{N_x}$, $d_y = \frac{L_y}{N_y}$. Finally, it will also be convenient to define the pixel aspect ratio $a_{y/x} = d_y/d_x$.

⁷In practice there may be dead space between the light sensitive regions. This would be important for calculating response to luminous flux. However, that does not matter for the geometrical issues considered in this document, so long as the pixels are evenly spaced.

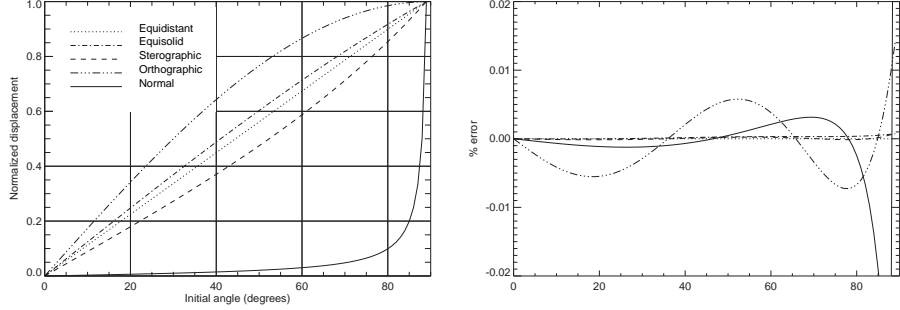


Figure 2: Left Panel: Plots of five ideal “fish-eye functions” mapping angle from optical axis to radial displacement. Right Panel: Errors in approximating functions with equation 39.

We will typically be interested in the location with respect to the CCD position corresponding to the “optical axis” (x_o, y_o) . Furthermore, it is more convenient to work with a dimensionless quantity produced by normalizing with pixel size. The resulting “pixel radius”

$$r_p = d/d_x = \sqrt{(x - x_o)^2 + a_{y/x}^2 (y - y_o)^2} \quad (40)$$

and “pixel angle”

$$\eta_p = \tan \left(a_{y/x} \frac{y - y_o}{x - x_o} \right) \quad (41)$$

are useful coordinates for relating CCD response to the optical system. Inverting these to recover pixel indices is straightforward

$$x = x_o + r_p \cos \eta_p \quad (42)$$

$$y = y_o + r_p \sin \eta_p \quad (43)$$

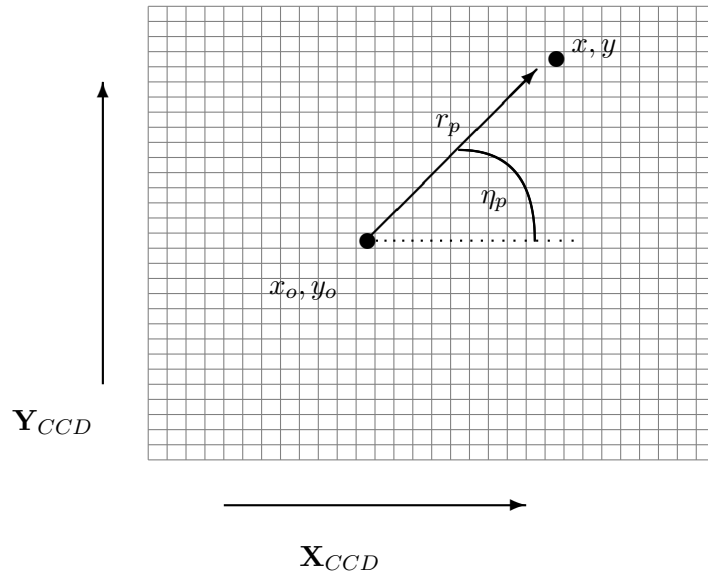


Figure 3: An illustration of the coordinate systems and conventions used for a CCD. The optical axis (x_0, y_0) is deliberately placed off-center. In practice it will be near, but not necessarily exactly at, the CCD center point.

2 Data

All-sky imagers typically use narrow band filters to isolate wavelengths of auroral interest while minimizing background contamination. The resulting images will contain light from celestial sources, but this may be obscured by auroral and airglow contributions. In addition to the auroral filters, many systems also take data using one or more background channels with passbands in spectral regions where no auroral luminosity is expected. These background channels are essential for accurate photometric work with faint emissions, but also produce useful “star frames”. NORSTAR ASIs typically have a background 2.0 nm filter centered at 480.0 nm (sometimes denoted as BACKGR). Exposures of a second or more at this wavelength will image several hundred stars if the viewing conditions are good. High-pass (near-infrared) and open filters may also be useful, although no data from these will be used for this report.

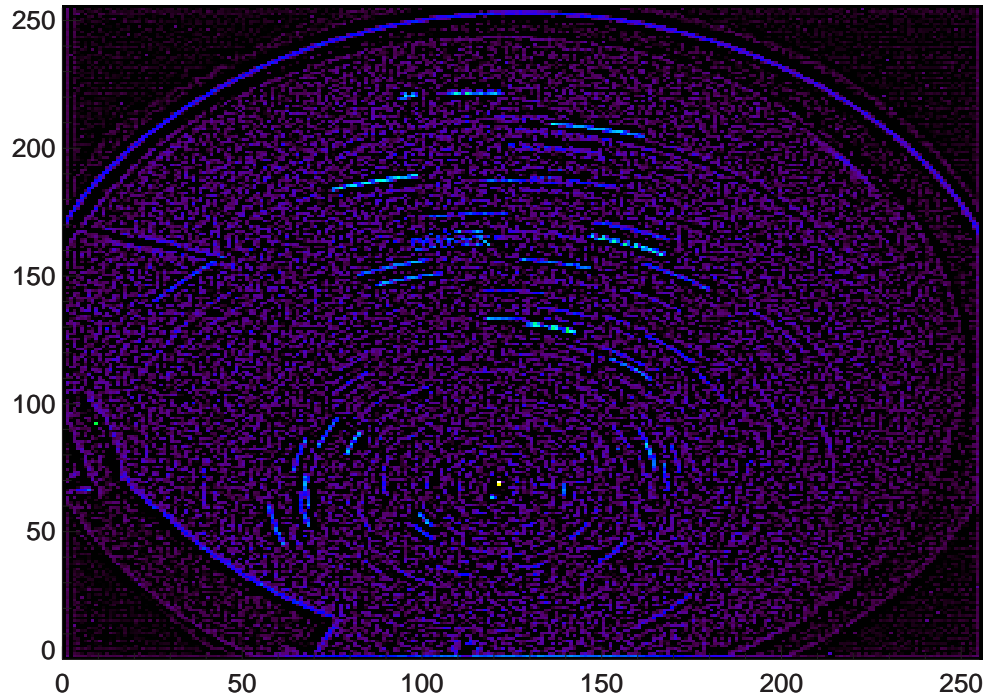


Figure 4: A one hour sequence with 59 background frames from Gillam during 06-07 UT December 21, 2001. Edge-enhancement has been used to emphasize star tracks. The Big Dipper is visible to the left of Polaris, which is a single bright point source at pixel coordinates 122,67. An overhead cable can be seen in the upper portion of the frame, with a GPS antenna and light-shield in the lower left corner.

3 Fitting

Three parameters are required to fully specify the instrument orientation, two more for the CCD alignment, and at least one more for the camera optics. Determining these six (or more) parameters is the central focus of this report. Previous sections contain all the information required to convert from pixel coordinates to a celestial reference frame. The problem is now to select a set of orientation and instrument parameters that is in some sense optimal. A practical solution requires the definition of some quality function which provides a quantifiable way of ranking results. Using this quality function, standard algorithms may be used to search for the “best” set of parameters. In practice it is relatively simple to find a good solution, but much harder to be sure that it is the best, as parameter space may contain many local minima, and convergence to a global minimum may be impossible to guarantee.

3.1 Initial Values

Parameter estimates can be determined from celestial sources with known locations. Initially, only sources at relatively small zenith angles ($< 45^\circ$) should be used. Working with low elevation targets may provide better constraints on camera orientation, but requires more complex models of the optical function. Unless there is a reason to do otherwise, it is useful to assume that the camera is roughly level, so $tilt = 0$, $pitch = 0$. In many cases the system will also be roughly north-south aligned, in which case $yaw \approx 0$.

```
;2002/05/08 This file created manually by Brian Jackel
;

instrument_name Polaris

site_name Gillam
site_code GILL

geodetic_latitude 56.38
geodetic_longitude 265.35

camera_yaw 0.0
camera_tilt 0.0
camera_pitch 0.0

optics_a1 1.48
optics_a2 0.0
optics_a3 0.0
optics_b1 0.0
optics_b2 0.0

ccd_x0 117.0
ccd_y0 122.0
```

Table 2: Camera parameters for Gillam estimated from a single star frame at 11:12 UT on December 23, 2001.

Viewed from Gillam, Polaris is nearly stationary at azimuth 0.0° and a zenith angle of 33.6° . Examination of a frame sequence from 2001/12/23 shows a peak brightness at approximately⁸ $x = 122, y = 67$. Eta Ursae Majoris is convenient as a second source, as it is easily identified (the last bright point in the handle of the Big Dipper) and travels over a useful range of sky. At 11:21 UT Eta Ursae Majoris was at pixel $x = 86, y = 117$ which should correspond to azimuth 90.1° and zenith angle 24.3° . Assuming approximate north-south alignment, the CCD position of the optical axis is $x_0 \approx 122, y_0 \approx 117$ and the first optical parameter is

$$a_1 \approx \frac{122 - 86}{24} \approx 1.5 \quad a_1 \approx \frac{117 - 67}{34} \approx 1.47 \quad (44)$$

⁸More precision could be obtained by fitting or centroiding, but that is not warranted at this stage.

so an initial value of 1.48 is not unreasonable. Using these values (summarized in Table 2) produces results shown in Figure 5, which are obviously smeared and offset from the correct locations. Using improved values (Table 3) gives the results in Figure 7 where stars are better localized and have offsets of less than a degree. However, other regions of the sky (not shown) still have small mapping errors.

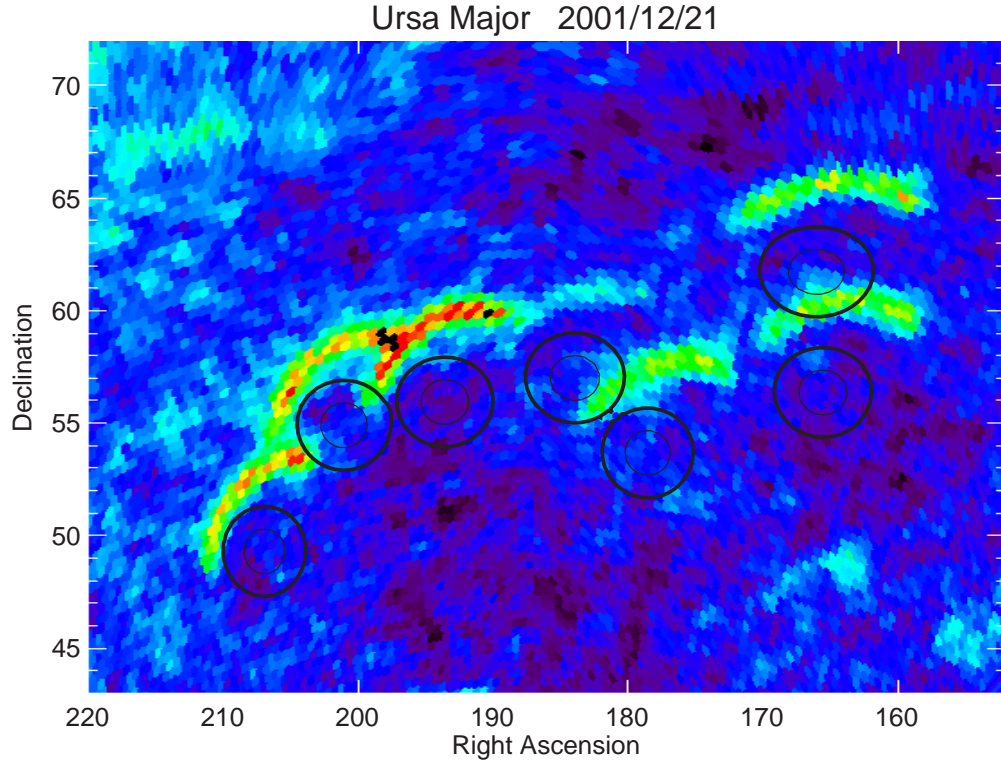


Figure 5: Composite image of the Big Dipper using parameters from Table 2.

3.2 Quality of Fit

Qualitative assessment of the results produced by any set of parameters is simple. Images projected into celestial coordinates are obviously “better” if stars are properly focused (Figure 7) and worse if stars are smeared or offset from their correct positions (Figure 5). Visual examination is sufficient for identifying a good fit and even for determining whether a change in parameters provides further improvement. Quantifying this is more difficult. Several methods were explored for this report, with the goal being to determine a robust and easily calculated quantity that accurately reflects the quality of a projection.

The current algorithm is encapsulated in the IDL program `asi_map_focus.pro` included in §6.3. It seems to work reasonably well, but could probably be improved.

3.3 Random Searching

As noted previously, there may not be a single global minimum. A general exploration of parameter space can help determine where local minima may be located, and validate the choice of initial parameters. Systematic searches of a d dimensional parameter space require $O(n^d)$ evaluations of the quality function, where n is the number of divisions per dimension. A comprehensive high-resolution multi-dimensional search may require unreasonable amounts of computing power. An alternative is to evaluate the quality function at random points in parameter space. Such a Monte Carlo search was carried out with 25,000 points over a wide range of parameters, with a subsequent 25,000 points over a smaller parameter range near the optimal fit. Results are shown in Figure 6. All parameters exhibit a clear single minimum.

While not as time consuming as an exhaustive search, this monte carlo survey required nearly 24 hours on a desktop computer. This is not an issue if parameter estimates only need to be re-determined for a few cameras each year. Increasing computational resources are likely to keep pace with expansion of the NORSTAR project; some improvements in code efficiency are also possible.

```
; c:\data\norstar\GILL\GILL_20010801_Polaris.asi_info
; Tue May 28 13:47:19 2002
; This file automatically generated by NORSTAR_INFO_WRITE
;
; **Best result from 50,000 random parameter sets **
;
do_not_use because_not_optimised
instrument_name Polaris
site_name Gillam
site_code GILL
geodetic_latitude      56.3800
geodetic_longitude     265.350
camera_yaw            2.13977
camera_tilt            1.48060
camera_pitch           -0.106570
optics_a1              1.45567
optics_a2              0.000000
optics_a3              0.000000
optics_b1              0.000000
optics_b2              0.000000
ccd_x0                122.172
ccd_y0                118.312
```

Table 3: Camera parameters for Gillam from a Monte Carlo search.

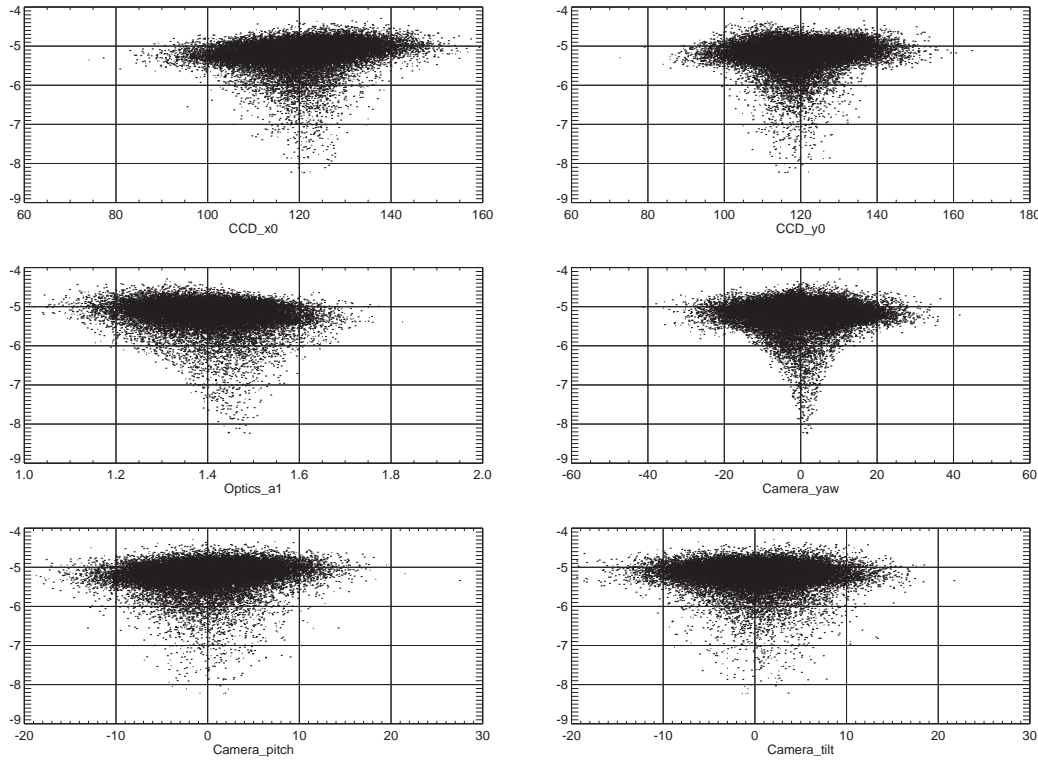


Figure 6: Results from a Monte Carlo search of 6-dimensional parameter space. Darker symbols are from the first stage of a wide search (25,000 points), lighter symbols from the second stage (25,000 points) concentrating on the region of best fit. Quality of fit is indicated on the y-axis, with small (more negative) numbers corresponding to better fits.

3.4 Systematic Optimization

There are many algorithms designed to search for minima in a multi-dimensional parameter space. The IDL routine amoeba [Press et al., 1997, see §10.4] was used for this report. This algorithm does not require derivatives, which are not directly available here and would have to be estimated numerically. It is not particularly efficient, but has proven to be extremely robust. Other, “better”, routines tended to proceed inappropriately when confronted with bad data. Such behavior is unacceptable for a final goal of automatic fitting without human intervention.

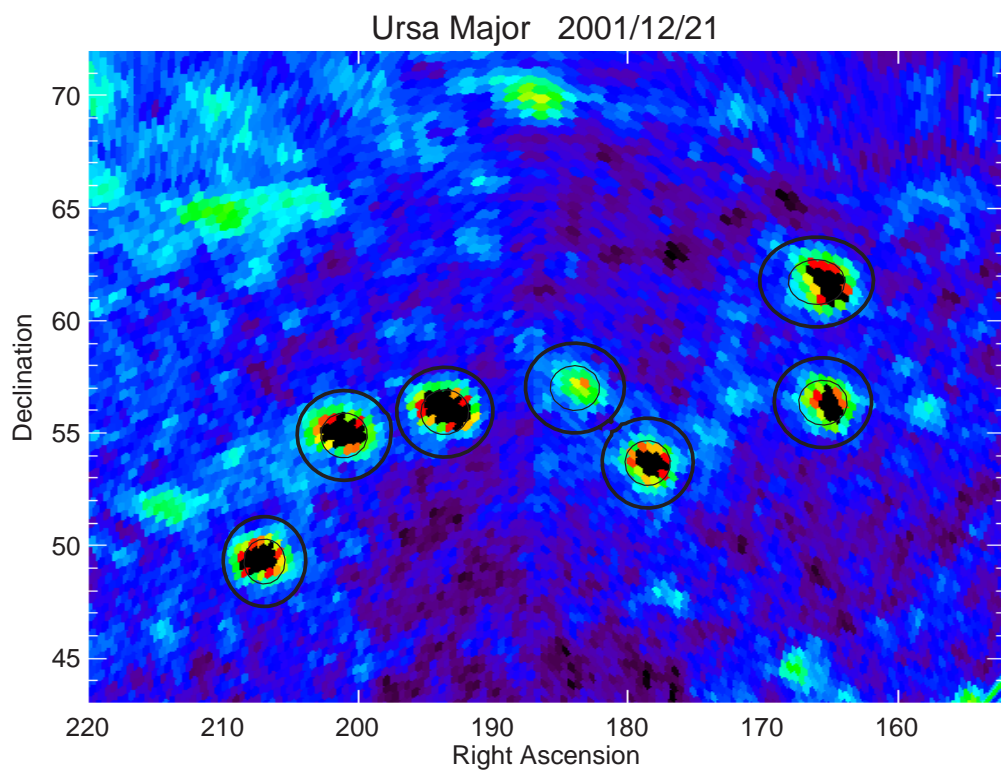


Figure 7: Projection of 54 background frames from 06-12UT 2001/12/21 onto a common GEI grid for the region containing Ursa Major. Pointing accuracy is on the order of $1/2^\circ$.

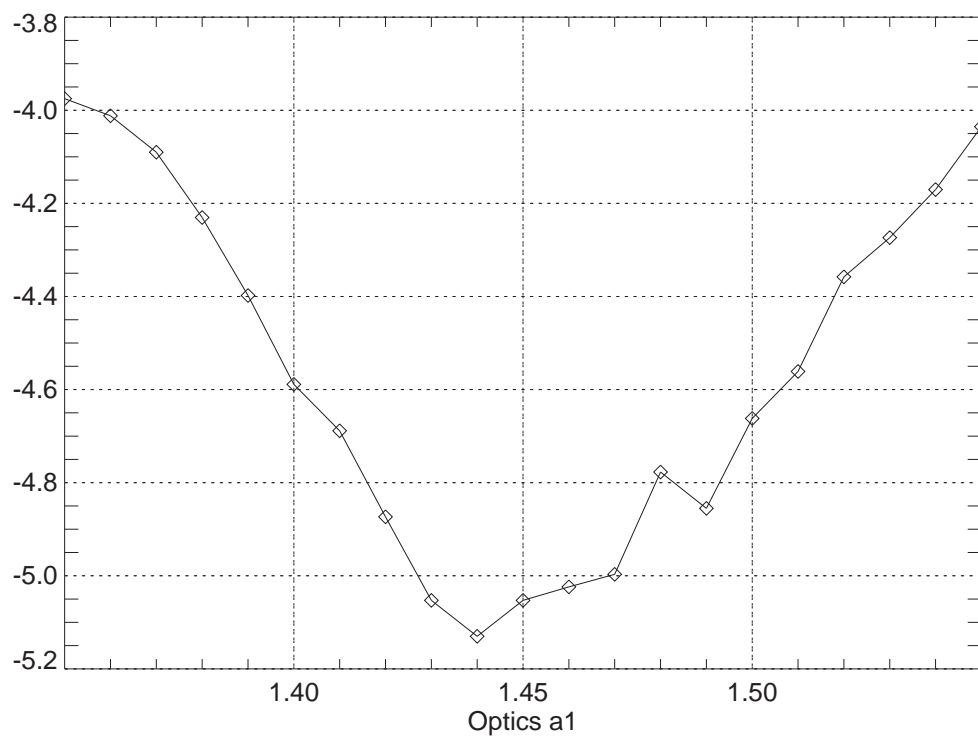


Figure 8: Quality of fit as a function of the optical parameter a_1 . There is an optimal minimum near $a_1 = 1.44$, but fitting algorithms may be confused by the local minimum at $a_1 = 1.49$.

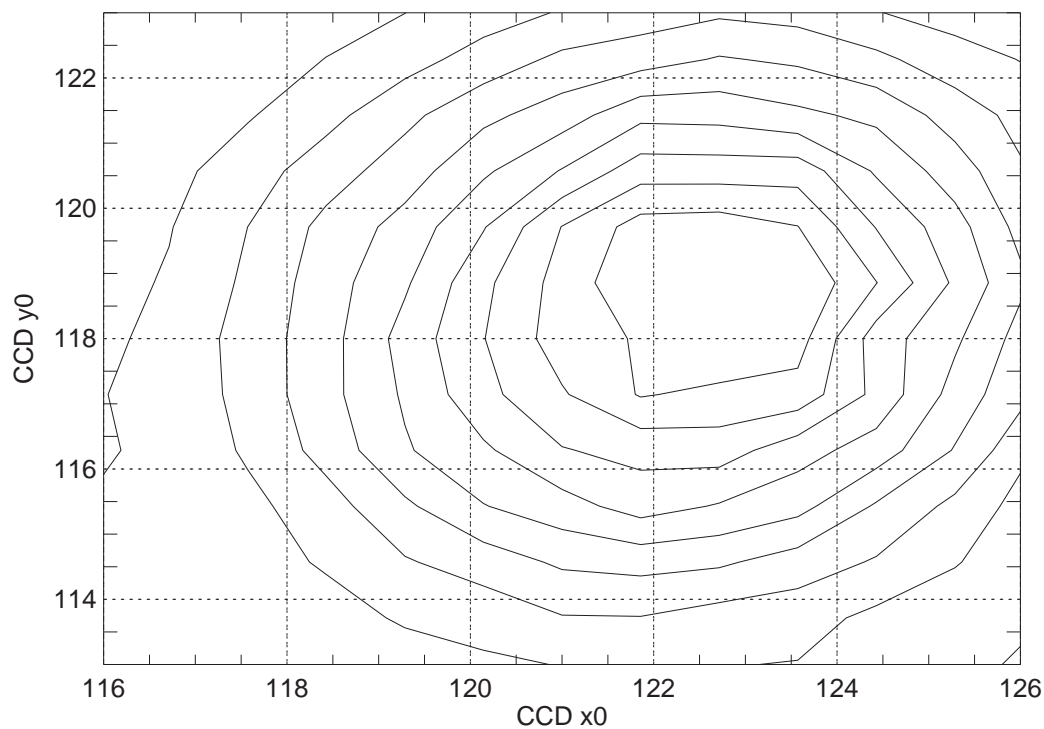


Figure 9: Contour plot of fit quality for various estimates of the CCD optical axis (x_0, y_0) . A clear minimum is evident near $(123, 119)$.

4 Viewing Conditions

If camera orientation and optical parameters are known, celestial sources may be used for other purposes. One particularly useful application is determination of viewing conditions, as clouds and haze will reduce or eliminate the photon flux from stars. A measure of star brightness relative to a surrounding star-free region consequently provides an indication of atmospheric transmission. This indicator can be determined automatically and may be sufficiently quantitative as to distinguish between clear sky, haze, and thin cloud. This is in contrast to visual examination of star frames, which is fundamentally qualitative and labor intensive.

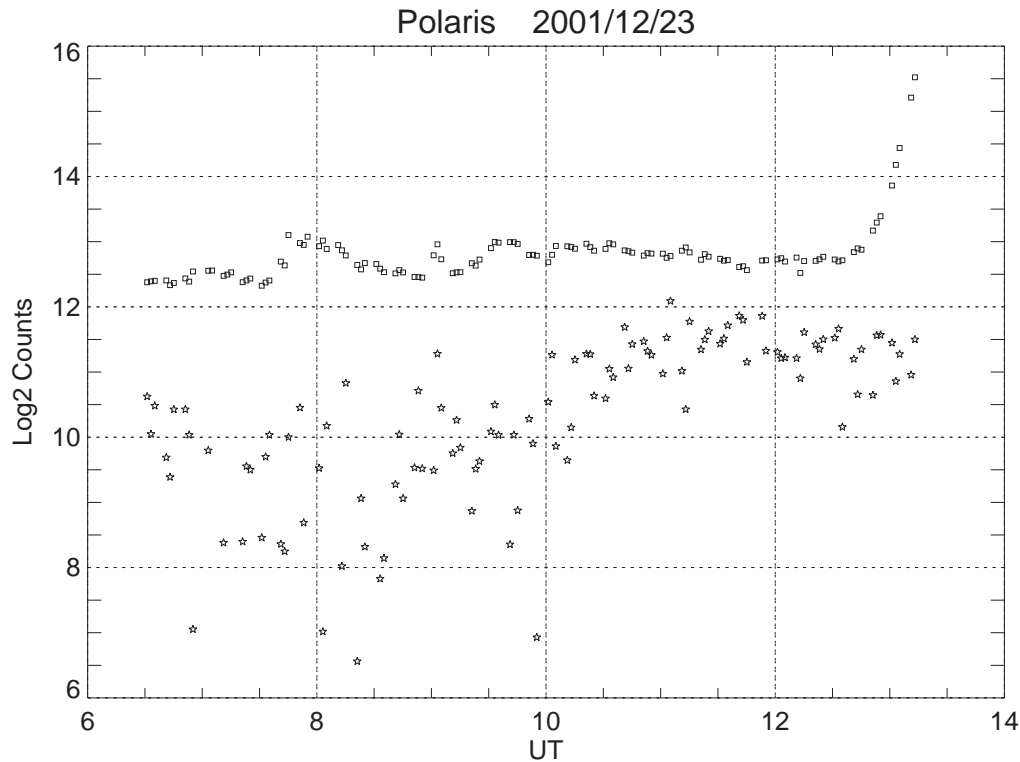


Figure 10: Background brightness (squares) and excess counts due to Polaris (stars).

Polaris is often used as a target for photometric determination of viewing conditions because it is essentially fixed in the sky and is isolated from other bright stars. These properties are also useful for ASI applications. Even without accurate knowledge of the camera optics and orientation, it is straightforward to identify the region of pixels containing Polaris, as well as an adjacent star-free region. Visual examination of a sequence of frames during several hours of 2001/12/23 suggests hazy conditions during the first few hours of this interval after which the sky appears to be clear. The sequence

of events is consistent with the time series shown in Figure 10.

The primary drawback of using Polaris is that it provides an indication of viewing conditions at only a single point. By using more stars it would be possible to obtain a full sky measure of visibility. This of course requires a sufficiently accurate knowledge of camera orientation and optics to track stars over the course of a night. It is also necessary to use only stars that are visible over the entire evening, or somehow account for their rising and setting.

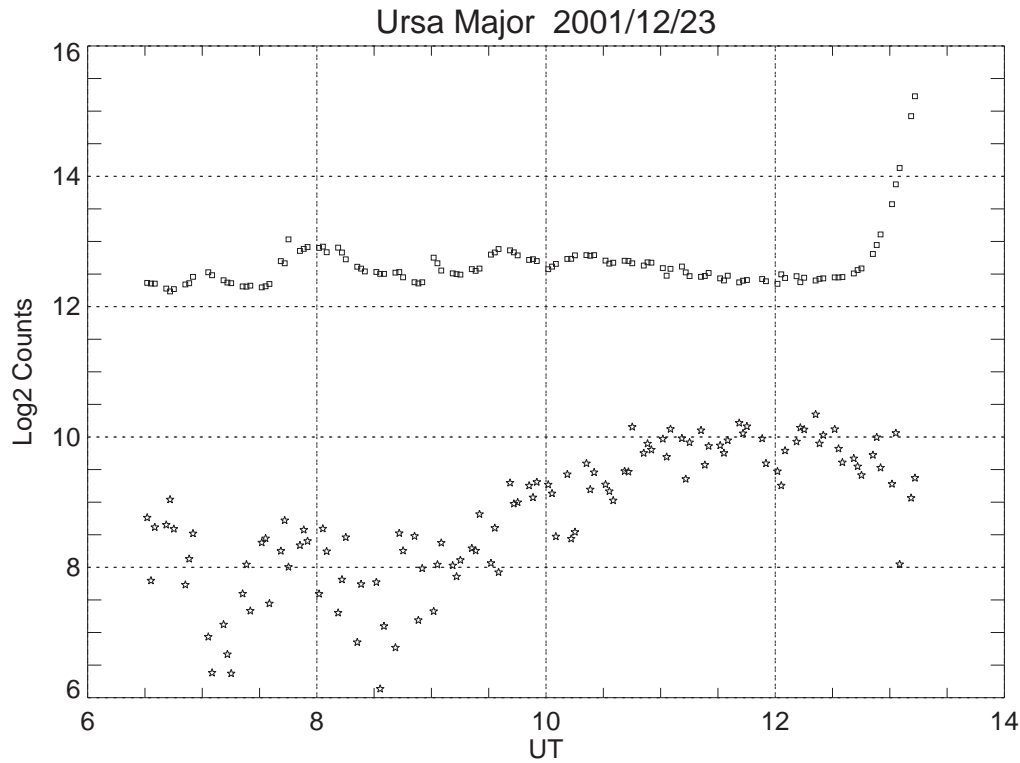


Figure 11: Background brightness and excess counts due to Ursa Major.

A test of feasibility was carried out with the “Big Dipper” (Ursa Major). Frames from the night of 2001/12/23 were projected onto a GEI grid with the average shown in figure 7. Star brightness was estimated by adding all values within 2° of the nominal star position. Background was determined from regions outside these boundaries. Results are shown in Figure 11, and are clearly similar to those in figure 10. However, using the Big Dipper provides an indication of viewing conditions over a much larger area ($16^\circ \times 16^\circ$) with enhanced signal-to-noise due to the larger number of sources. Increased spatial coverage could be obtained by increasing the number of target stars.

5 Summary

This report contains all the information required to project ASI frames into celestial coordinates. When combined with a measure of fit quality, this allows orientation and other instrument characteristics to be determined with a minimum of human intervention. Estimates of viewing conditions can also be obtained automatically.

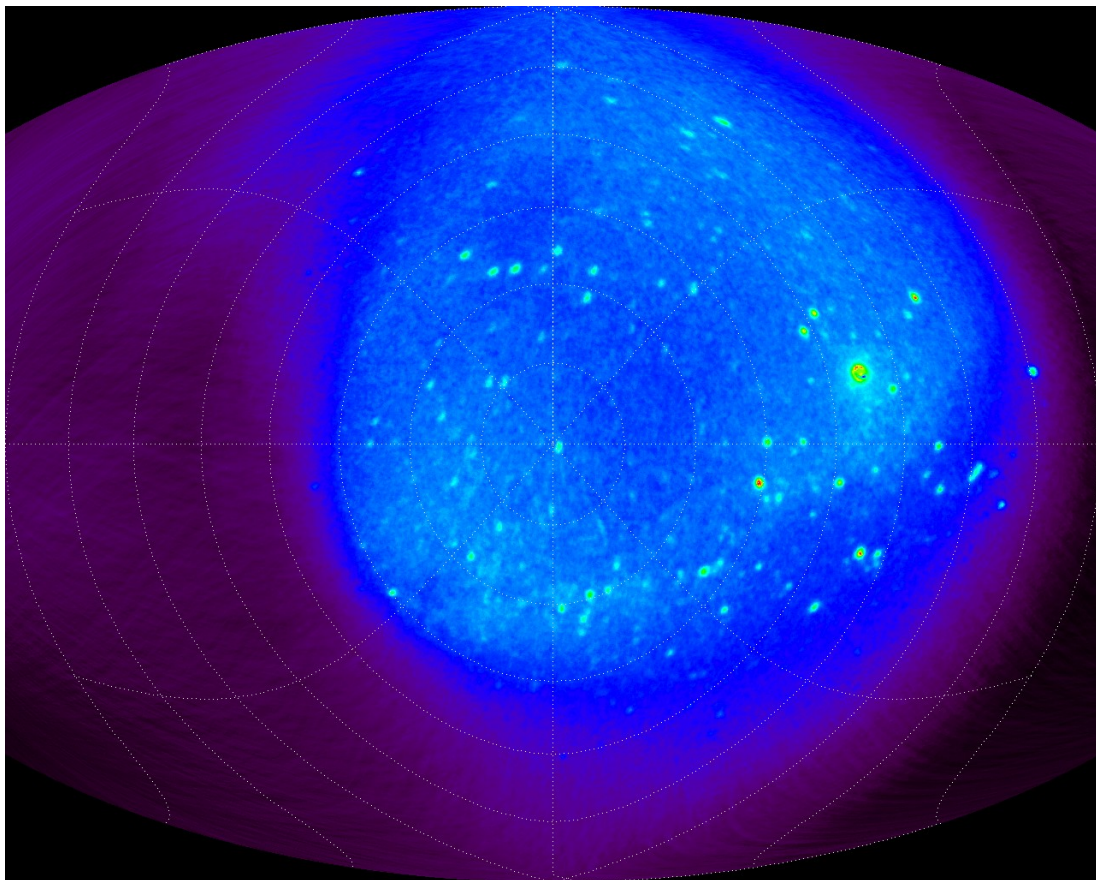


Figure 12: Composite image of the Big Dipper using parameters from Table 2.

5.1 Suggested Implementation

Preliminary estimates of instrument parameters should be obtained from visual examination of single star frames in combination with *a priori* knowledge. Results should be confirmed with an exhaustive monte-carlo search throughout a wide region of parameter space. Next, systematic searching would be used to determine optimal parameters.

This should be repeated using several different initial conditions in order to avoid local minima. Finally, large scale composite star maps should be created to verify the global quality of fit. Figure 12 contains an example of such a global fit based on the parameters in Table 3. Quality of focus is fairly good in most regions of the sky, but stars near the horizon are slightly smeared. Some improvement is clearly possible.

6 Additional Information

6.1 Jupiter

Ephemeris Generator at <http://ssd.jpl.nasa.gov/cgi-bin/eph>

Ephemeris Settings

```
Target Body: Planet Jupiter
Observer Location: User Specified Location
Coordinates: 26521'00.0''E, 5622'48.0''N, 100 m

From: A.D. 2001-12-23 00:00 UT
To: A.D. 2001-12-24 00:00
Step: 1 hour
Format: Calendar Date and Time

Output Quantities: 1-2,4,9,13
Ref. Frame, RA/Dec Format: J2000, Degrees
Apparent Coordinates Model: Refracted
```

HORIZONS Generated Ephemeris

```
*****
Ephemeris / WWW_USER Thu May 2 13:28:23 2002 Pasadena, USA / Horizons
*****
Target body name: Jupiter (599) {source: JUP172}
Center body name: Earth (399) {source: DE-0406LE-0406}
Center-site name: (User Defined Site)
*****
Start time : A.D. 2001-Dec-23 00:00:00.0000 UT
Stop time : A.D. 2001-Dec-24 00:00:00.0000 UT
Step-size : 60 minutes
*****
Center geodetic : 265.350000, 56.380000, 0.10000 {E-lon(deg),Lat(deg),Alt(km)}
Center cylindric: 265.35000, 3539.746, 5288.066 {E-lon(deg),Dxy(km),Dz(km)}
Center pole/equ : Standard Earth Model {East-longitude +}
Center radii : 6378.1 x 6378.1 x 6356.8 km {Equator, meridian, pole}
Target pole/equ : IAU_JUPITER {East-longitude -}
Target radii : 71492.0 x 71492.0 x 66854.0 km {Equator, meridian, pole}
Target primary : Sun {source: DE-0406LE-0406}
Interfering body: MOON (Req= 1737.400) km {source: DE-0406LE-0406}
Deflecting body : Sun, EARTH {source: DE-0406LE-0406}
Deflecting GMs : 1.3271E+11, 3.9860E+05 km^3/s^2
Atmos refraction: YES (Earth refraction model)
RA format : DEG
Time format : CAL
Units conversion: 1 AU= 149597870.691 km, c= 299792.458 km/s, 1 day= 86400.0 s
Table cut-offs 1: Elevation (-90deg=NO), Airmass (>38.0000=NO), Daylight (NO)
Table cut-offs 2: Solar Elongation ( -0.180.0=NO)
*****
Date__(UT)__HR:MN R.A._(J2000.0)_DEC R.A._(r-appar)_DEC. Azi_(r-appr)_Elev APmag S-brt Ang-diam
*****
2001-Dec-23 00:00 Am 102.87442 22.89190 102.85492 22.96131 64.3035 10.6700 -2.71 5.34 46.966
2001-Dec-23 01:00 m 102.86853 22.89252 102.86780 22.93046 76.1262 18.4603 -2.71 5.32 46.967
2001-Dec-23 02:00 m 102.86260 22.89313 102.87165 22.91734 88.2070 26.6817 -2.71 5.34 46.968
2001-Dec-23 03:00 m 102.85665 22.89375 102.87208 22.91072 101.1642 34.9599 -2.71 5.38 46.969
2001-Dec-23 04:00 m 102.85068 22.89436 102.87086 22.90718 115.8477 42.8420 -2.71 5.38 46.970
2001-Dec-23 05:00 m 102.84469 22.89496 102.86877 22.90537 133.3412 49.6934 -2.71 5.34 46.972
2001-Dec-23 06:00 m 102.83869 22.89555 102.86622 22.90468 154.5632 54.6042 -2.71 5.31 46.973
2001-Dec-23 07:00 102.83267 22.89614 102.86345 22.90485 178.9560 56.5217 -2.71 5.34 46.974
2001-Dec-23 08:00 102.82666 22.89672 102.86067 22.90579 203.5046 54.8920 -2.71 5.38 46.975
2001-Dec-23 09:00 102.82065 22.89729 102.85807 22.90758 225.0457 50.1921 -2.71 5.38 46.976
2001-Dec-23 10:00 102.81465 22.89785 102.85591 22.91045 242.8240 43.4641 -2.71 5.34 46.977
2001-Dec-23 11:00 102.80866 22.89841 102.85456 22.91498 257.6983 35.6410 -2.71 5.31 46.978
2001-Dec-23 12:00 102.80269 22.89896 102.85476 22.92243 270.7636 27.3776 -2.71 5.34 46.979
2001-Dec-23 13:00 A 102.79675 22.89951 102.85815 22.93593 282.8913 19.1377 -2.71 5.38 46.980
2001-Dec-23 14:00 N 102.79083 22.90006 102.86975 22.96549 294.7167 11.2987 -2.71 5.38 46.981
2001-Dec-23 15:00 * 102.78492 22.90061 102.91385 23.06217 306.6984 4.2532 -2.71 5.34 46.983
2001-Dec-23 16:00 * 102.77904 22.90116 103.08706 23.49299 319.1498 -1.3803 -2.71 5.31 46.984
2001-Dec-23 17:00 * 102.77318 22.90172 103.00150 23.51986 332.2281 -6.0722 -2.71 5.35 46.985
2001-Dec-23 18:00 * 102.76732 22.90229 102.90141 23.53942 345.9023 -9.0472 -2.71 5.38 46.986
2001-Dec-23 19:00 *m 102.76147 22.90287 102.79272 23.54700 359.9426 -10.0730 -2.71 5.38 46.987
2001-Dec-23 20:00 *m 102.75562 22.90345 102.68401 23.54069 13.9844 -9.0625 -2.71 5.34 46.988
2001-Dec-23 21:00 *m 102.74976 22.90405 102.58381 23.52236 27.6622 -6.1015 -2.71 5.31 46.989
```

```

2001-Dec-23 22:00 Cm 102.74388 22.90465 102.49813 23.49669 40.7451 -1.4214 -2.71 5.35 46.990
2001-Dec-23 23:00 Nm 102.73799 22.90526 102.67006 23.06827 53.2003 4.2046 -2.71 5.38 46.991
2001-Dec-24 00:00 Am 102.73207 22.90587 102.71469 22.97162 65.1838 11.2424 -2.71 5.38 46.992
*****
Column meaning:

```

TIME

Prior to 1972, times are UT1. Dates thereafter are UTC. Any 'b' symbol in the 1st-column denotes a B.C. date. First-column blank (" ") denotes an A.D. date. Calendar dates prior to 1582-Oct-15 are in the Julian calendar system. Later calendar dates are in the Gregorian system.

The uniform Coordinate Time scale is used internally. Conversion between CT and the selected non-uniform UT output scale has not been determined for UTC times after the next July or January 1st. The last known leap-second is used over any future interval.

NOTE: "n.a." in output means quantity "not available" at the print-time.

SOLAR PRESENCE

Time tag is followed by a blank, then a solar-presence symbol:

```

'*' Daylight (refracted solar upper-limb on or above apparent horizon)
'C' Civil twilight/dawn
'N' Nautical twilight/dawn
'A' Astronomical twilight/dawn
' ' Night OR geocentric ephemeris

```

LUNAR PRESENCE

The solar-presence symbol is immediately followed by a lunar-presence symbol:

```

'm' Refracted upper-limb of Moon on or above apparent horizon
' ' Refracted upper-limb of Moon below apparent horizon OR geocentric
      ephemeris

```

R.A._(J2000.0)_DEC. =
J2000.0 astrometric right ascension and declination of target. Corrected for light-time. Units: DEGREES

R.A._(r-appar)_DEC. =
Refracted apparent right ascension and declination of the target with respect to the Earth's true-equator and the meridian containing the Earth's true equinox-of-date. Corrected for light-time, the gravitational deflection of light, stellar aberration, precession, nutation and approximate atmospheric refraction. Units: DEGREES

Azi_(r-appr)_Elev =
Refracted apparent azimuth and elevation of target. Corrected for light-time, the gravitational deflection of light, stellar aberration, precession, nutation and approximate atmospheric refraction. Azimuth measured North(0) -> East(90)-> South(180) -> West(270), elevation with respect to plane perpendicular to local zenith direction. TOPOCENTRIC ONLY. Units: DEGREES

APmag S-brt =
Target's approximate apparent visual magnitude & surface brightness. Planet & satellite values are available for Earth or Moon observing sites only. Values for the Sun, comets and asteroids ARE available for non-Earth sites. Units: NONE & VISUAL MAGNITUDES PER SQUARE ARCSECOND

Ang-diam =
The equatorial angular width of the target body full disk, if it were fully visible to the observer. Units: ARCSECONDS

Computations by ...
Solar System Dynamics Group, Horizons On-Line Ephemeris System
4800 Oak Grove Drive, Jet Propulsion Laboratory
Pasadena, CA 91109 USA
Information: <http://ssd.jpl.nasa.gov/>
Connect : telnet://ssd.jpl.nasa.gov:6775 (via browser)
 telnet ssd.jpl.nasa.gov 6775 (via command-line)
Author : Jon.Giorgini@jpl.nasa.gov

```
*****

```

Credits/Awards

Contact: Webmaster (webmaster@ssd.jpl.nasa.gov)

Last modified: 2001 November 6 16:20

6.2 Bright Stars

Name	Catalog Number	Right Ascension	Declination	Visual Magnitude
Alp UMi	424	37.953	89.264	2.02
Bet UMi	5563	222.676	74.156	2.08
Alp Cep	8162	319.645	62.586	2.44
Alp UMa	4301	165.932	61.751	1.79
Gam Cas	264	14.177	60.717	2.47
Bet Cas	21	2.295	59.150	2.27
Alp Cas	168	10.127	56.537	2.23
Bet UMa	4295	165.460	56.382	2.37
Eps UMa	4905	193.507	55.960	1.77
Zet UMa	5054	200.981	54.925	2.27
Gam UMa	4554	178.457	53.695	2.44
Gam Dra	6705	269.152	51.489	2.23
Alp Per	1017	51.081	49.861	1.79
Eta UMa	5191	206.885	49.313	1.86
Alp Aur	1708	79.173	45.998	0.08
Alp Cyg	7924	310.358	45.280	1.25
Bet Aur	2088	89.882	44.947	1.90
Gam1And	603	30.975	42.330	2.26
Bet Per	936	47.042	40.956	2.12
Gam Cyg	7796	305.557	40.257	2.20
Alp Lyr	7001	279.235	38.784	0.03
Bet And	337	17.433	35.621	2.06
Eps Cyg	7949	311.553	33.970	2.46
Alp Gem	2891	113.650	31.888	1.98
Alp And	15	2.097	29.091	2.06
Bet Tau	1791	81.573	28.608	1.65
Bet Peg	8775	345.944	28.083	2.42
Bet Gem	2990	116.329	28.026	1.14
Alp CrB	5793	233.672	26.715	2.23
	5958	239.876	25.920	2.00
Alp Ari	617	31.793	23.462	2.00
Alp Boo	5340	213.915	19.183	-0.04
Alp Tau	1457	68.980	16.509	0.85
Gam Gem	2421	99.428	16.399	1.93
Alp Peg	8781	346.190	15.205	2.49
Bet Leo	4534	177.265	14.572	2.14
Alp Oph	6556	263.734	12.560	2.08
Alp Leo	3982	152.093	11.967	1.35
Eps Peg	8308	326.047	9.875	2.39
Alp Aql	7557	297.696	8.868	0.77
Alp Ori	2061	88.793	7.407	0.50
Gam Ori	1790	81.283	6.350	1.64
Alp CMi	2943	114.825	5.225	0.38
Del Ori	1852	83.002	0.299	2.23
Eps Ori	1903	84.053	-1.202	1.70
Zet Ori	1948	85.190	-1.943	2.05
Bet Ori	1713	78.635	-8.202	0.12
Alp Hya	3748	141.897	-8.659	1.98
Kap Ori	2004	86.939	-9.670	2.06
Alp Vir	5056	201.298	-11.161	0.98
Eta Oph	6378	257.595	-15.725	2.43
Alp CMa	2491	101.287	-16.716	-1.46
Bet CMa	2294	95.675	-17.956	1.98
Bet Cet	188	10.898	-17.987	2.04

Table 4: Sources from the Yale Bright Star Catalog with visual magnitudes less than 2.5, sorted by declination. Particularly bright sources are marked with gray shading. Sources with declinations less than -20° are not included.

6.3 IDL Code

asi_map_init.pro

```

RETURN
END ;-----



;----- PRO ASI_MAP_FRAME_LOAD year,month,day,hour,MMS_REGEX=mms_regex
COMMON ASIMAP_FRAME,nframes,frame_nx,frame_ny,frame,frame_yndims
COMMON ASIMAP_SITE
FORMAT=(/c:/data/norstar",A,".14.4,I2.2,"A,"_,-,I4.4,I2.2,I2.2,')
frame_nx= 256
frame_ny= 256
sitecode= site_asinfo.site_code
dataadir= STRING sitecode,year,month,sitecode,year,month,day,$
COMMON ASIMAP_FRAME,nframes,frame_nx,frame_ny,frame,frame_yndims
frame_nx= FILEINDI('*.png',dir,gridadir,depth,2)
IF (N_ELEMENTS(nsstars) GT 0) THEN BEGIN
  grid_ybsc.angle= 90.0
  FOR Index=0 TO nsstars-1 DO BEGIN
    r= star_ras[Index]*dotor & d= star_declinat*!dotor
    star_gsi= (COS(r)*COS(d), SIN(r)*COS(d), SIN(d))
    star_gsi= REFORM(star_gsi,1,3)
    star_gsi= REBLIN(star_gsi,grid_nx*grid_ny*grid_ny*grid_ybsc.angle < ABS(ACOS(TOTAL(star_gsi*grid,2)))
  ENDFOR
  grid_ybsc.angle= grid_ybsc.angle//!dotor
  grid_yras= ATAN(grid[*,1]/grid[*,0])//!dotor
  grid_xras= (grid_ras+360.0) MOD 360.0
  grid_yras= ATAN(grid[*,2]/SQR((grid[*,0]^2+grid[*,1]^2)))//!dotor
  grid_xras= REFORM(grid_xras,grid_nx,grid_ny,ngrids)
  ENDIF
END ;-----



;----- PRO ASI_MAP_FRAME2GRID,asidata
COMMON ASIMAP_GRID
grid.frame= UNTARR(grid_nx*grid_ny*ngrids,nframes)
FOR Ind=0 TO nframes-1 DO BEGIN
  pix= ASI_MAP_GE2CD(grid,asidata,frame_ydmst*,indx*)
  pix= REFORM(frame*,indx)
  tmp= pix[*,0]
  pix= pix[*,*]
  pix= pix[*,*]
  on_ccc= (pix[*,*] GE 0) AND (pix[*,*] LE frame_ny)
  grid_frame[0,indx]= ccc*(on_ccd EQ 1)
ENDFOR
RETURN
END ;-----



FUNCTION ASI_MAP_FOCUS,asidata,ALLINFO=allinfo
COMMON ASIMAP_FRAME
grid.frame= TOTAL(grid.frame,2)/nframes
average= MIN(average)
tmp= average / TOTAL(tmp)
weight= (grid_ybsc.angle > 5.0) - 5.0
weight= (ABS(grid_ybsc.angle) < 5.0) - 5.0
allinfo.aim= TOTAL(tmp*(grid_ybsc.angle+1.0))
stop= 0.0d0
FOR Ind=0 TO nframes-1 DO BEGIN
  blur= TOTAL(blur + (grid.frame[* ,indx] - average)^2)
ENDFOR
allinfo.aim= TOTAL(blur/(TOTAL(blur)))
allinfo.blur= blur/(TOTAL(blur))
average56= BYTE(SORT(average))
allinfo.entropy= SYMBOL.ENTROPY(average256)
S= SORT(average)
S$= strpoints[0..95]
allinfo.range= average[S]
RETURN allinfo.aim
END
END ;----- Wrapper for "map_set" and also stores the lat/lon for each pixel.
grid= TRANPOSE(grid,[0..2,1])

```

```

; This is moderately time consuming but only needs to be done once.
; for each protection and/or window size.

PRO ASI_MAP_SET_POLT_POLON_ROT {EXTRA= extra
COMMON ASI_MAP_SIT map_set_info [ ] ; On
SEEN_POLT_POLON_ROT EXTRA= extra
nx= 1.6 X size /size /size /size
ny= 1.6 Y size /size /size /size
xx= INGEN(nx) # REPLICATE (nx)
yy= REPLICATE(1,ny)
map_set_Position= CONVERT_COORD_xx_yy /DEVICE ,/TO_DATA)
map_set_Position= TRANPOSE(map_set_Position)
RETURN
END ;-----



PRO ASI_MAP_TOOLS_TEST
COMMON ASIMAP_STAR
COMMON ASIMAP_SITE
COMMON ASIMAP_FRAME
COMMON ASIMAP_GRID
ASI_MAP_STAR_LOAD 'gill' ,2001 ,12 ,23
ASI_MAP_SITE_LOAD 'gill' ,2001 ,12 ,23
ASI_MAP_FRAME_LOAD 'gill' ,2001 ,12 ,23
ASI_MAP_GRID_LOAD 'gill' ,2001 ,12 ,23
ASI_MAP_FRAME2GRID 'gill' ,site_asinInfo
STOP
RETURN
END ;-----



PRO ASI_MAP_TEST
COMMON ASIMAP_SITE
COMMON ASIMAP_FRAME
COMMON ASIMAP_GRID
ASI_MAP_SIT 45,-180,65 /HAMMER ,/GRID ,LIMIT=[ 50 , -120 , 75 , -40 ], /CONTINENT
map_set_Position[* ,2]= 120.0d3
img_TRYED()
cc0= ASI_MAP_POS2CCD(map_set_position ,site_info ,zenith ,angle )
view= WHERE[ (cc0[* ,0]^gr0)^AND (cc0[* ,1]^gr1)^AND (cc0[* ,2]^gr2)^AND (cc0[* ,3]^gr3)^AND (cc0[* ,4]^gr4)^AND (cc0[* ,5]^gr5)^AND (cc0[* ,6]^gr6)^AND (cc0[* ,7]^gr7)^AND (cc0[* ,8]^gr8)^AND (cc0[* ,9]^gr9)^AND (cc0[* ,10]^gr10)^AND (cc0[* ,11]^gr11)^AND (cc0[* ,12]^gr12)^AND (cc0[* ,13]^gr13)^AND (cc0[* ,14]^gr14)^AND (cc0[* ,15]^gr15)^AND (cc0[* ,16]^gr16)^AND (cc0[* ,17]^gr17)^AND (cc0[* ,18]^gr18)^AND (cc0[* ,19]^gr19)^AND (cc0[* ,20]^gr20)^AND (cc0[* ,21]^gr21)^AND (cc0[* ,22]^gr22)^AND (cc0[* ,23]^gr23)^AND (cc0[* ,24]^gr24)^AND (cc0[* ,25]^gr25)^AND (cc0[* ,26]^gr26)^AND (cc0[* ,27]^gr27)^AND (cc0[* ,28]^gr28)^AND (cc0[* ,29]^gr29)^AND (cc0[* ,30]^gr30)^AND (cc0[* ,31]^gr31)^AND (cc0[* ,32]^gr32)^AND (cc0[* ,33]^gr33)^AND (cc0[* ,34]^gr34)^AND (cc0[* ,35]^gr35)^AND (cc0[* ,36]^gr36)^AND (cc0[* ,37]^gr37)^AND (cc0[* ,38]^gr38)^AND (cc0[* ,39]^gr39)^AND (cc0[* ,40]^gr40)^AND (cc0[* ,41]^gr41)^AND (cc0[* ,42]^gr42)^AND (cc0[* ,43]^gr43)^AND (cc0[* ,44]^gr44)^AND (cc0[* ,45]^gr45)^AND (cc0[* ,46]^gr46)^AND (cc0[* ,47]^gr47)^AND (cc0[* ,48]^gr48)^AND (cc0[* ,49]^gr49)^AND (cc0[* ,50]^gr50)^AND (cc0[* ,51]^gr51)^AND (cc0[* ,52]^gr52)^AND (cc0[* ,53]^gr53)^AND (cc0[* ,54]^gr54)^AND (cc0[* ,55]^gr55)^AND (cc0[* ,56]^gr56)^AND (cc0[* ,57]^gr57)^AND (cc0[* ,58]^gr58)^AND (cc0[* ,59]^gr59)^AND (cc0[* ,60]^gr60)^AND (cc0[* ,61]^gr61)^AND (cc0[* ,62]^gr62)^AND (cc0[* ,63]^gr63)^AND (cc0[* ,64]^gr64)^AND (cc0[* ,65]^gr65)^AND (cc0[* ,66]^gr66)^AND (cc0[* ,67]^gr67)^AND (cc0[* ,68]^gr68)^AND (cc0[* ,69]^gr69)^AND (cc0[* ,70]^gr70)^AND (cc0[* ,71]^gr71)^AND (cc0[* ,72]^gr72)^AND (cc0[* ,73]^gr73)^AND (cc0[* ,74]^gr74)^AND (cc0[* ,75]^gr75)^AND (cc0[* ,76]^gr76)^AND (cc0[* ,77]^gr77)^AND (cc0[* ,78]^gr78)^AND (cc0[* ,79]^gr79)^AND (cc0[* ,80]^gr80)^AND (zangle LE 80.0)

```

References

- Herbert Goldstein. *Classical mechanics*. Addison-Wesley Series in Physics. Addison-Wesley, 2nd edition, 1980.
- M.A. Hapgood. Space physics coordinate transformations: a users guide. *Planet. Space Sci.*, 40:711–717, 1992.
- C. Jekeli. Geodesy and gravity. In Adolph S. Jursa, editor, *Handbook of Geophysics and The Space Environment*, chapter 24. Air Force Geophysics Laboratory, 1985.
- Kenneth R. Lang. *Astrophysical Formulae: A compendium fo the Physicist and Astronomer*. Springer-Verlag, 2nd edition, 1980.
- William H. Press, Saul A. Teukolsky, William T. Vetterling, and Brian P. Flannery. *Numerical Recipes in C*. Cambridge University Press, 2nd edition, 1997.